Transport in Porous Media **43:** 557–580, 2001.

Water Injection into a Low-Permeability Rock - 2: Control Model

DMITRIY B. SILIN[1] and TAD W. PATZEK[1,2]
[1]*Lawrence Berkeley National Laboratory, 1 Cyclotron Rd, MS 90-1116, Berkeley, CA 94720, U.S.A.*
[2]*University of California, Berkeley, Materials Science and Mineral Engineering, 591 Evans Hall, Berkeley, CA 94720-1760, U.S.A.*

(Received: 30 June 1999; in final form: 16 August 2000)

Abstract. In Part 1, we have demonstrated the inevitable growth of the fluid injection hydrofractures in low-permeability rocks. Thus, a smart controller that manages fluid injection in the presence of hydrofracture extension is highly desirable. Such a controller will be an essential part of automated waterflood project surveillance and control. Here we design an optimal injection controller using methods of optimal control theory. The controller inputs are the history of the injection pressure and the cumulative injection, along with the fracture size. The output parameter is the injection pressure and the control objective is the injection rate. We demonstrate that the optimal injection pressure depends not only on the instantaneous measurements, but it is determined by the whole history of the injection and of the fracture area growth. We show the controller robustness when the inputs are delayed and noisy and when the fracture undergoes abrupt extensions. Finally, we propose a procedure that allows estimation of the hydrofracture size at no additional cost.

Key words: waterflood, hydrofracture, optimal injection, controller, quadratic optimization.

Nomenclature

A	fracture face effective area, m^2.
k	absolute rock permeability, md, 1 md $\approx 9.87 \times 10^{-16}$ m^2.
k_{rw}	relative permeability of water.
p_i	initial pressure in the formation outside the fracture, Pa.
p_{inj}	injection pressure, Pa.
q	injection rate, 1/Day.
Q	cumulative injection, 1.
v	superficial leak-off velocity, m/day.
w	fracture width, m.
α_w	water hydraulic diffusivity, m^2/Day.
μ	viscosity, Pa-s.

1. Introduction

Our ultimate purpose is to design an integrated system of field-wide waterflood surveillance and supervisory control. As of now, this system consists of Waterflood Analyzer (De and Patzek, 1999) and a network of individual injector controllers,

all implemented in modular software. In this paper, we design an optimal controller of water injection into a low permeability rock through a hydrofractured well. We control the water injection rate as a prescribed function of time and regulate the wellhead injection pressure. The controller is based on the optimization of a quadratic performance criterion subject to the constraints imposed by a model of the injection well-hydrofracture-formation interactions. The input parameters are the injection pressure, the cumulative volume of injected fluid and the area of injection hydrofracture. The output is the injection pressure, and the objective of the control is a prescribed injection rate that may be time-dependent. We show that the optimal output depends not only on the instantaneous measurements, but also on the entire history of measurements.

The wellhead injection pressures and injection rates are readily available if the injection water pipelines are equipped with pressure gauges and flow meters, and the respective measurements are appropriately collected and stored as time series. The cumulative injection is then calculated from a straightforward integration. The controller processes the data and outputs the appropriate injection pressure. In an ideal situation, it can be used 'on line', that is, be implemented as an automatic device. But it also can be used as a tool to determine the injection pressure which can be applied through manual regulation. Automation of the process of data collection and control leads to a better definition of the controller and, therefore, reduces the risk of a catastrophic fracture extension.

Measurements of the hydrofracture area are less easily available. Holzhausen and Gooch (1985), Ashour and Yew (1996), and Patzek and De (1998) have developed a *hydraulic impedance* method of characterizing injection hydrofractures. This method is based on the generation of low frequency pressure pulses at the wellhead or beneath the injection packer, and on the subsequent analysis of acoustic waves returning from the wellbore and the fracture. Wright and Conant, (1995) use tiltmeter arrays to estimate the fracture orientation and growth. An up-to-date overview of hydrofracture diagnostics methods has been presented by Warpinski (1996).

The controller input requires an effective fracture area rather than its geometric structure, see (Patzek and Silin, 2001). The effective fracture area implicitly incorporates variable permeability of the surrounding formation, and it also accounts for the decrease of permeability caused by formation plugging. To identify the effective fracture area, we propose in the present paper to utilize the system response to the controller action. For this purpose one needs to maintain a database of injection pressure and cumulative injection which are collected anyway. Hence, the proposed method does not impose any extra measurement costs, whereas the other methods listed above are quite expensive.

In Part 1 of this paper, we have considered a model of transient fluid injection into a low-permeability rock through a vertical hydrofracture. We arrived at a model describing transient fluid injection into a very low permeability reservoir, for example, diatomite or chalk, for several years. We have modified the original

Carter's model (Howard and Fast, 1957) of transient leak-off from a hydrofracture to account for the initial fracture area. We also have extended Carter's model to admit variable injection pressure and transformed it to an equivalent simpler form. As a result, we have arrived at a Volterra integral convolution equation expressing the cumulative fluid injection through the history of injection pressure and the fracture area (Patzek and Silin, 2001), Equation (24).

The control procedure is designed in the following way. First, we determine what cumulative injection (or, equivalently, injection rate) is the desirable goal. This decision can be made through waterflood analysis (De and Patzek, 1999), reservoir simulation and economics, and it is beyond the scope of this paper. Second, we reformulate the control objective in terms of the cumulative injection. Since the latter is just the integral of injection rate, this reformulation imposes no additional restrictions. Then, by analyzing the deviation of the actual cumulative injection from the target cumulative injection, and using the measured fracture area, the controller determines injection pressure, which minimizes this deviation. Control is applied by adjusting a flow valve at the wellhead and it is iterated in time, see Figure 1.

The convolution nature of the model does not allow us to obtain the optimal solution as a genuine feedback control and to design the controller as a standard closed-loop system. At each time, we have to account for the previous history of injection. However, the feedback mode may be imitated by designing the control on a relatively short time interval, which slides with time. When an unexpected event happens, for example, a sudden fracture extension occurs, a new sliding interval is generated and the controller is refreshed promptly.

A distinctive feature of the controller proposed here is that the injection pressure is computed through a model of the injection process. Although we cannot predict when and how the fracture extensions happen, the controller automatically takes

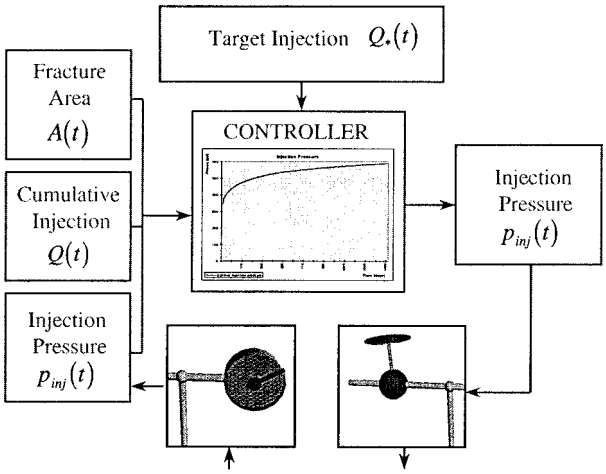

Figure 1. The controller scheme.

into account the effective fracture area changes and the decrease of the pressure gradient caused by the saturation of the surrounding formation with the injected water. Here we present the theoretical background of the controller. Its practical implementation and engineering may require additional considerations on a case-by-case basis.

This paper is organized as follows. First we overview the modified Carter's model of hydrofracture growth; for details we refer the reader to Part 1 (Patzek and Silin, 2001). Second, we derive the system of equations characterizing the optimal injection pressure. Third, we discuss how this system of equations can be solved for different models of fracture growth. Fourth, we obtain and compare three modes of optimal control: exact optimal control, optimal control produced by the system of equations, and piecewise-constant optimal control. Finally, we present several examples. The optimal injection pressure is computed through the minimization of a quadratic performance criterion using optimal control theory methods. Therefore, a considerable part of the paper is devoted to the development of mathematical background.

2. Theory

2.1. MODIFIED CARTER'S MODEL

We assume transient linear flow from a vertical fracture through which an incompressible fluid (water) is injected into the surrounding formation. The flow is orthogonal to the fracture faces. The fluid is injected under a pressure $p_{\text{inj}}(t)$ which is uniform inside the fracture but may depend on time t. Under these assumptions, the cumulative injection can be calculated from the following equation (Patzek and Silin, 2001):

$$Q(t) = wA(t) + 2\frac{kk_{\text{rw}}}{\mu\sqrt{\pi\alpha_w}}\int_0^t \frac{(p_{\text{inj}}(\tau) - p_i)A(\tau)}{\sqrt{t-\tau}}\,\mathrm{d}\tau. \tag{1}$$

Here k and k_{rw} are, respectively, the absolute rock permeability and the relative water permeability in the formation outside the fracture, and μ is the water viscosity. Parameters α_w and p_i denote the constant* hydraulic diffusivity and the initial pressure in the formation. The effective fracture area at time t is measured as $A(t)$ and its effective width is denoted by w. The coefficient 2 in Equation (1) reflects the fact that a fracture has two faces of approximately equal areas, so the total fracture surface area is equal to $2\,A(t)$. The first term on the right-hand side of Equation (1) represents the portion of the injected fluid spent on filling up the fracture volume. It is small in comparison with the second term in (1). We assume that the permeability inside the fracture is much higher than outside it, so at any time variation of the injection pressure throughout the fracture is negligibly small. We introduce $A(t)$ as an effective area because the actual permeability may change in time because of formation plugging (Barkman and Davidson, 1972) and changing water saturation.

* In the future, hydraulic diffusivity can be made time-dependent.

It follows from (1) that the initial value of the cumulative injection is equal to $wA(0)$. The control objective is to keep the injection rate $q(t)$ as close as possible to a prescribed target injection rate $q_*(t)$. Since Equation (1) is formulated in terms of cumulative injection, it will be more convenient to formulate the optimal control problem in terms of target cumulative injection

$$Q_*(t) = Q_*(0) + \int_0^t q_*(\tau)\,\mathrm{d}\tau. \tag{2}$$

If control maintains the actual cumulative injection close to $Q_*(t)$, then the actual injection rate is close to $q_*(t)$ on average.

To formulate an optimal control problem, we need to select a performance criterion for the process described by (1). Suppose that we are planning to apply control on a time interval $[\vartheta, T]$, $T > \vartheta \geqslant 0$. In particular, this means that the cumulative injection and the injection pressure are known on the interval $[0, \vartheta]$, along with the effective fracture area function $A(t)$. On the interval $[\vartheta, T]$ we want to apply such an injection pressure that the resulting cumulative injection will be as close as possible to (2). This requirement may be formulated in the following way:

Minimize

$$\begin{aligned} J[p_{\mathrm{inj}}] \;=\; & \frac{1}{2}\int_\vartheta^T w_q(t)(Q(t) - Q_*(t))^2\,\mathrm{d}t + \\ & + \frac{1}{2}\int_\vartheta^T w_p(t)(p_{\mathrm{inj}}(t) - p_*(t))^2\,\mathrm{d}t, \end{aligned} \tag{3}$$

subject to constraint (1).

The weight functions w_p and w_q are positive-defined. They reflect trade-off between the closeness of the actual cumulative injection $Q(t)$ to the target $Q_*(t)$, and the well-posedness of the optimization problem. For small values of w_p, minimization of functional (3) enforces $Q(t)$ to follow the target injection strategy $Q_*(t)$. However, if the value of w_p becomes too small, then the problem of minimization of functional (3) becomes ill-posed (Tikhonov and Arsenin, 1977, Vasil'ev, 1982). Moreover, in the equation characterizing the optimal control, derived below, the function w_p is in the denominator, which means that computational stability of this equation deteriorates as w_p approaches zero. At the same time, if we consider a specific mode of control, for example, piecewise constant control, then the well-posedness of the minimization problem is not affected if $w_p \equiv 0$. The function $p_*(t)$ defines a reference value of the injection pressure. Theoretically this function can be selected arbitrarily; however, practically it is better if it gives a rough estimate of the optimal injection pressure. Below, we discuss the ways in which $p_*(t)$ can be reasonably specified.

The optimization problem we just have formulated is a linear-quadratic optimal control problem. In the next section, we derive the necessary and sufficient conditions of optimality in the form of a system of integral equations.

2.2. OPTIMAL INJECTION PRESSURE

2.2.1. *Control Model*

Here we obtain necessary and sufficient optimality conditions for problem (1)–(3). We analyze the obtained equations in order to characterize optimal control in two different modes: the continuous mode and the piecewise-constant mode. Also, we characterize the injection pressure function, which provides exact identity $Q(t) \equiv Q_*(t)$, $\vartheta \leqslant t \leqslant T$.

Put $U(t) = p_{\text{inj}}(t) - p_*(t)$ and $V(t) = Q(t) - Q_*(t)$, $\vartheta \leqslant t \leqslant T$. Then the optimal control problem transforms into

minimize

$$J = \frac{1}{2}\int_{\vartheta}^{T} w_q(t)V(t)^2\,\mathrm{d}t + \frac{1}{2}\int_{\vartheta}^{T} w_p(t)U(t)^2\,\mathrm{d}t, \tag{4}$$

subject to

$$\begin{aligned} V(t) \;=\; & -Q_*(t) + wA(t) + 2\frac{kk_{\text{rw}}}{\mu\sqrt{\pi}\alpha_w}\int_0^{\vartheta}\frac{(p_{\text{inj}}(\tau) - p_i)A(\tau)}{\sqrt{t-\tau}}\,\mathrm{d}\tau + \\ & + 2\frac{kk_{\text{rw}}}{\mu\sqrt{\pi\alpha_w}}\int_{\vartheta}^{t}\frac{U(\tau)A(\tau)}{\sqrt{t-\tau}}\,\mathrm{d}\tau. \end{aligned} \tag{5}$$

In this setting, the control parameter is function $U(t)$. We have deliberately split the integral over $[0, t]$ into two parts in order to single out the only term depending on the control parameter $U(t)$.

A perturbation $\delta U(t)$ of the control parameter $U(t)$ on the interval $[\vartheta, T]$ produces variation of functional (4) and constraint (5):

$$\delta J = \int_{\vartheta}^{T} w_q(t)V(t)\delta V(t)\,\mathrm{d}t + \int_{\vartheta}^{T} w_p(t)U(t)\delta U(t)\,\mathrm{d}t, \tag{6}$$

$$\delta V(t) - 2\frac{kk_{\text{rw}}}{\mu\sqrt{\pi\alpha_w}}\int_{\vartheta}^{t}\frac{A(\tau)}{\sqrt{t-\tau}}\delta U(\tau)\,\mathrm{d}\tau = 0. \tag{7}$$

The integral in (7) is taken only over $[\vartheta, T]$ because the control $U(t)$ is perturbed only on this interval and, by virtue of (5), this perturbation does not affect $V(t)$ on $[0, \vartheta]$. Using the standard Lagrange multipliers technique (Vasil'ev, 1982), we infer that the minimum of functional (4) is characterized by the following equation:

$$U(t) = -2\frac{kk_{\text{rw}}}{\mu\sqrt{\pi\alpha_w}w_p(t)}A(t)\int_t^T\frac{w_q(\tau)}{\sqrt{\tau-t}}V(\tau)\,\mathrm{d}\tau, \qquad \vartheta \leqslant t \leqslant T. \tag{8}$$

Taking (5) into account and passing back to the original variables, we obtain that the optimal injection pressure $p_0(t)$ and the cumulative injection $Q_0(t)$ are provided

by solving the following system of equations:

$$Q_0(t) = wA(t) + 2\frac{kk_{\mathrm{rw}}}{\mu\sqrt{\pi\alpha_w}}\int_0^{\vartheta}\frac{(p_{\mathrm{inj}}(\tau)-p_i)A(\tau)}{\sqrt{t-\tau}}\,\mathrm{d}\tau + \\ +2\frac{kk_{\mathrm{rw}}}{\mu\sqrt{\pi\alpha_w}}\int_{\vartheta}^{t}\frac{(p_0(\tau)-p_i)A(\tau)}{\sqrt{t-\tau}}\,\mathrm{d}\tau, \tag{9}$$

$$p_0(t) = p_*(t) - 2\frac{kk_{\mathrm{rw}}}{\mu\sqrt{\pi\alpha_w}w_p(t)}A(t)\times \\ \times\int_t^T\frac{w_q(\tau)}{\sqrt{\tau-t}}(Q_0(\tau)-Q_*(\tau))\,\mathrm{d}\tau, \qquad \vartheta\leqslant t\leqslant T. \tag{10}$$

2.2.2. *Model Analysis*

The importance of a nonzero weight function $w_p(t)$ is obvious from Equation (10). The injection pressure, that is, the controller output is not defined if $w_p(t)$ is equal to zero.

Equation (10), in particular, implies that the optimal injection pressure satisfies the condition $p_0(T) = p_*(T)$. This is an artifact caused by the integral quadratic criterion (3) affecting the solution in a small neighborhood of T, but it makes important the appropriate selection of the function $p_*(T)$. For example, the trivial function $p_*(t) \equiv 0$ is not a good choice of the reference function in (3) because it enforces zero injection pressure by the end of the current subinterval. A rather simple and reasonable selection is provided by $p_*(t) \equiv P_*$, where P_* is the optimal constant pressure on the interval $[\vartheta, T]$. The equation characterizing P_* will be obtained below, see Equation (21).

Notice that the optimal cumulative injection $Q_0(t)$ depends on the entire history of injection pressure up to time t. Also, the optimal injection pressure is determined by Equation (10) on the entire time interval $[\vartheta, T]$. This feature prohibits a genuine closed loop feedback control mode. However, there are several ways to circumvent this difficulty.

First, we can organize the process of control as a step-by-step procedure. We split the whole time interval into reasonably small pieces, so that on each interval we can expect that the formation properties do not change too much. Then we compute the optimal injection pressure for this interval and apply it at the well-head by adjusting the control valve. As soon as either the measured cumulative injection or the fracture begins to deviate from the estimates, which were used to determine the optimal injection pressure, the control interval $[\vartheta, T]$ has to be refreshed. It also means that we must revise the estimate of the fracture area $A(t)$ for the refreshed interval and the expected optimal cumulative injection. Thus, the control is designed on a sliding time interval $[\vartheta, T]$. Other useful trick is to refresh the control interval before the current interval expires even if the measured and

computed parameters stay in good agreement. Computer simulations show that even a small overlap of the subsequent control intervals considerably improves the controller performance. This modification simplifies the choice of the function $p_*(t)$ in Equation (3), because the condition $p_0(T) = p_*(T)$ plays an important role only in a small neighborhood of the endpoint T.

Another manner of obtaining the optimal control from Equation (10) is to change the model of fracture growth. So far, we have treated the fracture as a continuously growing object. It is clear, however, that the area of the fracture may grow in steps. This observation leads to the piecewise-constant fracture growth model. We can design our control assuming that the fracture area is constant on the current interval $[\vartheta, T]$. If independent measurements tell us that the fracture area has changed, the interval $[\vartheta, T]$ and the control must be refreshed immediately. Equations (9) and (10) are further simplified and the optimal solution can be obtained analytically for a piecewise constant fracture growth model, see Equation (36) below.

Before proceeding further, let us make a remark concerning the solvability of the system of integral Equations (9)–(10). For simplicity let us assume that both weight functions w_p and w_q are constant. In this case, one may note that the integral operators on the right-hand sides of (9) and (10) are adjoint to each other. More precisely, if we define an integral operator

$$Df(\cdot)(t) = 2\frac{kk_{\mathrm{rw}}}{\mu\sqrt{\pi\alpha_w}}\int_{\vartheta}^{t}\frac{f(\tau)A(\tau)}{\sqrt{t-\tau}}\,\mathrm{d}\tau, \tag{11}$$

then its adjoint operator is equal to

$$D^*g(\cdot)(t) = 2\frac{kk_{\mathrm{rw}}}{\mu\sqrt{\pi\alpha_w}}A(t)\int_{\vartheta}^{t}\frac{g(\tau)}{\sqrt{t-\tau}}\,\mathrm{d}\tau. \tag{12}$$

The notation $Df(\cdot)$ means that operator D transforms the whole function $f(t)$, $\vartheta \leqslant t \leqslant T$, rather than its particular value, into another function defined on $[\vartheta, T]$, and $Df(\cdot)(t)$ denotes the value of that other function at t. The notation $D^*g(\cdot)(t)$ is similar.

If both weight functions $w_p(t)$ and $w_q(t)$ are constant, then the system of Equations (9), (10) can be expressed in the operator form as

$$\begin{aligned} Q &= DP + b_Q, \\ P &= -\frac{w_q}{w_p}D^*Q + b_P, \end{aligned} \tag{13}$$

where

$$b_Q(t) = wA(t) + 2\frac{kk_{\mathrm{rw}}}{\mu\sqrt{\pi\alpha_w}}\int_{0}^{\vartheta}\frac{(p_{\mathrm{inj}}(\tau) - p_i)A(\tau)}{\sqrt{t-\tau}}\,\mathrm{d}\tau, \tag{14}$$

$$b_P(t) = p_*(t) + 2\frac{w_q}{w_p}\frac{kk_{\mathrm{rw}}}{\mu\sqrt{\pi\alpha_w}}A(t)\int_t^T \frac{1}{\sqrt{\tau - t}}Q_*(\tau)\,\mathrm{d}\tau \tag{15}$$

and Q and P denote, respectively, the cumulative injection and injection pressure on the interval $[\vartheta, T]$. From (13) one deduces the following equation with one unknown function P

$$\left(D^*D + \frac{w_p}{w_q}\,\mathrm{Id}\right)P = -D^*b_Q + \frac{w_p}{w_q}b_P, \tag{16}$$

where Id is the identity operator. The operator inside the brackets on the left-hand side of (16) is self-adjoint and positive-definite. Therefore, the solution to Equation (16) can be efficiently obtained, say, with a conjugate gradient algorithm. Note that as the ratio w_p/w_q increases, the term $w_p/w_q\,\mathrm{Id}$ dominates (16), and Equation (16) becomes better posed. When $w_p = 0$, the second term in functional (4) must be dropped and in order to solve (16) one has to invert a product of two Volterra integral operators. Zero belongs to the continuous spectrum of operator D (Kolmogorov and Fomin, 1975) and, therefore, the problem of inversion of such an operator might be ill-posed.

In the discretized form, the matrix that approximates operator D is lower triangular; however, the product D^*D does not necessarily have a sparse structure. The above mentioned ill-posedness of the inversion of D manifests itself by the presence of a row of zeros in its discretization. Thus, for the discretized form we obtain the same rule: the larger the ratio w_p/w_q is, the better posed is Equation (16). However, if w_p/w_q is too large, then criterion (4) estimates the deviation of the injection pressure from $p_*(t)$ on $[\vartheta, T]$ rather than the ultimate objective of the controller. A reasonable compromise in selecting the weights w_p and w_q, that provides well-posedness of the system of integral Equations (9) and (10) without a substantial deviation from the control objectives, should be found empirically.

2.3. PIECEWISE CONSTANT INJECTION PRESSURE

In this section, the control is a piecewise-constant function of time. This means that the whole time interval, on which the injection process is considered, is split into subintervals with a constant injection pressure on each of them. The simplicity of the optimal control obtained under such assumptions makes it much easier to implement in practice. However, piecewise constant structure of admissible control definitely may deteriorate the overall performance in comparison with the class of arbitrary admissible controls. At the same time, an arbitrary control can be approximated by a piecewise-constant control with any accuracy as the longest interval of constancy goes to zero.

In order to avoid cumbersome calculations, we further assume that the injection pressure is constant on entire sliding interval $[\vartheta, T]$ introduced in the previous sec-

tion. Denote by P the value of the injection pressure on $[\vartheta, T]$. Then Equation (1) reduces to

$$Q(t) = wA(t) + 2\frac{kk_{\mathrm{rw}}}{\mu\sqrt{\pi\alpha_w}}\int_0^{\vartheta}\frac{(p_{\mathrm{inj}}(\tau)-p_i)A(\tau)}{\sqrt{t-\tau}}\,\mathrm{d}\tau + \\ + 2\frac{kk_{\mathrm{rw}}}{\mu\sqrt{\pi\alpha_w}}\int_{\vartheta}^{t}\frac{A(\tau)}{\sqrt{t-\tau}}\,\mathrm{d}\tau(P-p_i). \tag{17}$$

Put

$$a_q(t) = 2\frac{kk_{\mathrm{rw}}}{\mu\sqrt{\pi\alpha_w}}\int_{\vartheta}^{t}\frac{A(\tau)}{\sqrt{t-\tau}}\,\mathrm{d}\tau \tag{18}$$

and

$$b_q(t) = wA(t) + 2\frac{kk_{\mathrm{rw}}}{\mu\sqrt{\pi\alpha_w}}\int_0^{\vartheta}\frac{(p_{\mathrm{inj}}(\tau)-p_i)A(\tau)}{\sqrt{t-\tau}}\,\mathrm{d}\tau. \tag{19}$$

In the case of constant injection pressure, the necessity of the regularization term in (3) is eliminated and one obtains the following optimization problem:

minimize the quadratic functional

$$J[P] = \frac{1}{2}\int_{\vartheta}^{T}(b_q(t) + a_q(t)(P-p_i) - Q_*(t))^2\,\mathrm{d}t, \tag{20}$$

among all constant injection pressures P.

Clearly, the solution to this problem is characterized by $J'[P] = 0$ and the optimal value P_* of the constant injection pressure on the interval $[\vartheta, T]$ is characterized by

$$P_* = p_i - \frac{\int_{\vartheta}^{T}(b_q(t) - Q_*(t))a_q(t)\,\mathrm{d}t}{\int_{\vartheta}^{T}a_q^2(t)\,\mathrm{d}t}. \tag{21}$$

Since the fracture area is always positive, the denominator in (21) is nonzero (cf. Equation (18)) and P_* is well defined. As above, in order to apply (21) one needs an estimate of the fracture area one the interval $[\vartheta, T]$, so this interval should not be too long, so that formation properties do not change considerably on it.

The obtained value P_* can be used to compute a more elaborate control strategy by solving (9), (10) for $p_*(t) \equiv P_*$ on $[\vartheta, T]$. Note that $b_q(t)$ is equal to the historic cumulative injection until $t \geqslant \vartheta$, through the part of the fracture, which opened by the time ϑ. If the actual cumulative injection follows the target injection closely enough, then the value of $b_q(t)$ should be less than $Q_*(t)$, so normally we should have $P_* > p_i$.

2.4. EXACT OPTIMIZATION

Another possibility to keep the injection rate at the prescribed level is to solve Equation (1) with $Q(t) = Q_*(t)$ on the left-hand side. Theoretically, the injection pressure obtained this way outperforms both the optimal pressure obtained by solving Equations (9) and (10), and the piecewise-constant optimal pressure. However, to compute the exactly optimal injection pressure one needs to know the derivative $\mathrm{d}A(t)/\mathrm{d}t$. Since measurements of the fracture area are never accurate, the derived error in estimating $\mathrm{d}A(t)/\mathrm{d}t$ will be large and probably unacceptable. However, we present the exactly optimal solution here because it can be used for reference and in *a posteriori* estimates.

In order to solve Equation (1) we apply the Laplace transform. Denote the solution to Equation (1) by $Q_*(t)$. Clearly, $Q_*(0) = wA(0)$. Put $A_1(t) = A(t) - A(0)$ and $Q_1(t) = Q_*(t) - Q_*(0)$ and denote by $f(t)$ the product $(p_{\mathrm{inj}}(t) - p_i)A(t)$. Hence, Equation (1) transforms into

$$Q_1(t) = wA_1(t) + 2\frac{kk_{\mathrm{rw}}}{\mu\sqrt{\pi\alpha_w}}\int_0^t \frac{f(\tau)}{\sqrt{t-\tau}}\,\mathrm{d}\tau. \tag{22}$$

Application of the Laplace transform to Equation (22) produces

$$L[Q_1](s) = wL[A_1](s) + 2\frac{kk_{\mathrm{rw}}}{\mu\sqrt{\pi\alpha_w}}\frac{\sqrt{\pi}}{\sqrt{s}}L[f](s). \tag{23}$$

Hence

$$2\frac{kk_{\mathrm{rw}}}{\mu\sqrt{\alpha_w}}\sqrt{\pi}L[f](s) = \frac{\sqrt{\pi}}{\sqrt{s}}(sL[Q_1](s) - wsL[A_1](s)). \tag{24}$$

From (24) one infers that

$$2\frac{kk_{\mathrm{rw}}}{\mu\sqrt{\alpha_w}}\sqrt{\pi}f(t) = \int_0^t \frac{\frac{\mathrm{d}}{\mathrm{d}\tau}(Q_1(\tau) - wA_1(\tau))}{\sqrt{t-\tau}}\,\mathrm{d}\tau. \tag{25}$$

In the original notation, (25) finally implies that

$$p_{\mathrm{inj}}(t) = p_i + \frac{\mu\sqrt{\alpha_w}}{2\sqrt{\pi}kk_{\mathrm{rw}}A(t)}\int_0^t \frac{q_*(\tau) - w\frac{\mathrm{d}A(\tau)}{\mathrm{d}\tau}}{\sqrt{t-\tau}}\,\mathrm{d}\tau. \tag{26}$$

Note that from (26)

$$p_{\mathrm{inj}}(0) = p_i. \tag{27}$$

Hence, the idealized exact optimal control assumes a gentle startup of injection. If both functions $q_*(t)$ and $\mathrm{d}A(t)/\mathrm{d}t$ are bounded, then for a small positive t the function $p_{\mathrm{inj}}(t)$ increases approximately proportionally to the square root of time.

If our intention is to keep the injection rate constant, $q_*(t) \equiv q_*$, then (26) further simplifies to

$$p_{\text{inj}}(t) = p_i + \frac{\mu\sqrt{\alpha_w}\sqrt{t}}{\sqrt{\pi}kk_{\text{rw}}A(t)}q_* - \frac{\mu\sqrt{\alpha_w}}{2\sqrt{\pi}kk_{\text{rw}}A(t)}w\int_0^t \frac{\frac{\mathrm{d}A(\tau)}{\mathrm{d}\tau}}{\sqrt{t-\tau}}\,\mathrm{d}\tau. \tag{28}$$

Without fracture growth, the last integral in (28) vanishes and the injection pressure increases proportionally to the square root of time. The pressure cannot increase indefinitely; at some point this inevitably will lead to a fracture extension. In addition, (27) and (28) imply that the optimal injection pressure cannot be constant for all times.

It is interesting to note that if $A(t) = \sqrt{at}$, see (Patzek and Silin, 2001), the integral in Equation (28) does not depend on t and we get

$$p_{\text{inj}}(t) = p_i + \frac{\mu\sqrt{\alpha_w}}{kk_{\text{rw}}\sqrt{\pi a}}q_* - \frac{\mu w\sqrt{\pi\alpha_w a}}{4kk_{\text{rw}}\sqrt{t}}. \tag{29}$$

Therefore, in this particular case the optimal injection pressure at constant injection rate q_* asymptotically approaches a constant value

$$p_\infty = p_i + \frac{\mu\sqrt{\alpha_w}}{kk_{\text{rw}}\sqrt{\pi a}}q_*, \quad \text{as} \quad t \to \infty. \tag{30}$$

2.5. PIECEWISE CONSTANT FRACTURE GROWTH MODEL

So far, the fracture growth has been continuous, providing a reasonable approximation at a large time scale. However, it is natural to assume that the fracture grows in small increments. As we mentioned above, constant fracture area stipulates increase of injection pressure (or injection rate decline that we are trying to avoid). An increase of the pressure results in a step-enlargement of the fracture. The latter, in turn, increases flow into the formation and causes a decrease of the injection pressure as the controller response. An increase of the flow rate causes an even bigger drop in the injection pressure because of the growing fracture area, and because the pressure gradient is greater on the faces of the recently opened portions of the fracture than in the older parts of the fracture. The injection rate starts to decrease due to the increasing formation pressure, this causes the controller to increase the injection pressure, and the process repeats in time.

We assume that considerable changes of the fracture area can be detected by observation. This implies that on the current interval, on which the controller is being designed, the fracture area can be handled as a constant. In other words, $A(t) \equiv A(\vartheta)$, $\vartheta \leqslant t \leqslant T$. Then the derivative of $A(t)$ is equal to a sum of Dirac's delta-functions

$$\frac{\mathrm{d}A(t)}{\mathrm{d}t} = \sum_{\vartheta_j < t} (A(\vartheta_j + 0) - A(\vartheta_j - 0))\delta(t - \vartheta_j), \tag{31}$$

where $A(-0) = 0$. It is not difficult to see that (1) transforms into

$$Q(t) = wA(\vartheta_K) + 2\frac{kk_{\rm rw}}{\mu\sqrt{\pi\alpha_w}} \sum_{\vartheta_j<t} A(\vartheta_j) \int_{\vartheta_j}^{T_j^{\rm end}} \frac{(p_{\rm inj}(\tau) - p_i)}{\sqrt{t-\tau}}\,{\rm d}\tau + \\ + 2\frac{kk_{\rm rw}}{\mu\sqrt{\pi\alpha_w}} A(\vartheta_K) \int_{\vartheta_K}^{t} \frac{(p_{\rm inj}(\tau) - p_i)}{\sqrt{t-\tau}}\,{\rm d}\tau, \tag{32}$$

where $[\vartheta_K, T_K]$ is the current sliding interval containing t. On the preceding interval $[0, \vartheta_K]$, the control was designed on the contiguous intervals $[\vartheta_j, T_j]$, $0 = \vartheta_0 < \vartheta_1 < \ldots < \vartheta_{K-1}$. As discussed above, the actual interval of application of the design control may be shorter than $[\vartheta_j, T_j]$. We denote it by $[\vartheta_j, T_j^{\rm end}]$, $\vartheta_j < T_j^{\rm end} \leqslant T_j$, so that $\vartheta_{j+1} = T_j^{\rm end}$ and every two consequent intervals are overlapping. The optimal continuous pressure $p_K(t)$ and respective cumulative injection $Q_K(t)$ defined on an interval $[\vartheta_K, T_K]$ are obtained from the solution of the following system of equations

$$Q_K(t) = wA(\vartheta_K) + 2\frac{kk_{\rm rw}}{\mu\sqrt{\pi\alpha_w}} \sum_{\vartheta_j<t} A(\vartheta_j) \int_{\vartheta_j}^{T_j^{\rm end}} \frac{(p_{\rm inj}(\tau) - p_i)}{\sqrt{t-\tau}}\,{\rm d}\tau + \\ + 2\frac{kk_{\rm rw}}{\mu\sqrt{\pi\alpha_w}} A(\vartheta_K) \int_{\vartheta_K}^{t} \frac{(p_K(\tau) - p_i)}{\sqrt{t-\tau}}\,{\rm d}\tau, \tag{33}$$

$$p_K(t) = p_*(t) - 2\frac{kk_{\rm rw}}{\mu\sqrt{\pi\alpha_w} w_p(t)} A(\vartheta_K) \times \\ \times \int_t^{T_K} \frac{w_q(\tau)}{\sqrt{t-\tau}} (Q_K(\tau) - Q_*(\tau))\,{\rm d}\tau,\ \vartheta_K < t \leqslant T_K. \tag{34}$$

Again, although $p_K(t)$ and $Q_K(t)$ are defined on the whole interval $[\vartheta_K, T_K]$, they are going to be applied on a shorter interval $[\vartheta_K, T_K^{\rm end}]$ and the new interval begins at $\vartheta_{K+1} = T_K^{\rm end}$. An important distinction between the systems of Equations (33), (34) and (9), (10) is that in (33) and (34) there is no dependence of the optimal injection pressure and the respective cumulative injection on the fracture area on $[\vartheta_K, T_K]$. On the other hand, the assumption of the constant area itself is an estimate of $A(t)$ on the interval $[\vartheta_K, T_K]$.

For the exactly optimal control, that is, the injection pressure which produces cumulative injection precisely coinciding with $Q_*(t)$, one obtains the following expression (see Equation (26)):

$$p_{\rm inj}(t) = p_i + \frac{\mu\sqrt{\alpha_w}}{2\sqrt{\pi}kk_{\rm rw}A(\vartheta_K)} \times \\ \times \left(\int_0^t \frac{q_*(\tau)}{\sqrt{t-\tau}}\,{\rm d}\tau - w \sum_{0<\vartheta_j<t} \frac{(A(\vartheta_j) - A(\vartheta_{j-1}))}{\sqrt{t-\vartheta_j}} \right), \tag{35}$$

where, again, $[\vartheta_K, T_K]$ is the first interval containing t. If, further, the target injection rate is constant on each interval, that is $q_*(t) \equiv q_{*j}$, $\vartheta_j < t \leqslant T_j^{\text{end}}$, then (35) transforms into

$$p_{\text{inj}}(t) = p_i + \frac{\mu\sqrt{\alpha_w}}{2\sqrt{\pi}kk_{\text{rw}}A(\vartheta_K)} \sum_{0<\vartheta_j<t} (2q_{*j}(\sqrt{t-\vartheta_{j-1}} - \sqrt{t-\vartheta_j}) - \\ - w(A(\vartheta_j) - A(\vartheta_{j-1}))/\sqrt{t-\vartheta_j}). \tag{36}$$

The respective cumulative injection in this case is

$$Q(t) = wA(\vartheta_K) + 2\frac{kk_{\text{rw}}}{\mu\sqrt{\pi\alpha_w}} \sum_{0<\vartheta_j<t} A(\vartheta_j) \int_{\vartheta_j}^{T_j^{\text{end}}} \frac{p_{\text{inj}}(\tau) - p_i}{\sqrt{t-\tau}}\,\mathrm{d}\tau + \\ + 2\frac{kk_{\text{rw}}}{\mu\sqrt{\pi\alpha_w}} A(\vartheta_K) \int_{\vartheta_K}^{t} \frac{p_{\text{inj}}(\tau) - p_i}{\sqrt{t-\tau}}\,\mathrm{d}\tau. \tag{37}$$

Note that it follows from (36) that at each instant ϑ_j of fracture growth there is a short in time, but large in magnitude pressure drop. In the piecewise constant model this drop is singular of order $O(1/\sqrt{t-\vartheta_j})$. Practically, even during gradual fracture extensions, if the area grows continuously at a high rate then the injection pressure drops sharply.

Further simplifications of the solution occur if the injection pressure is piecewise constant as well. We adjust the sliding intervals to the intervals where the injection pressure is constant. Equation (1) then transforms into

$$Q(t) = wA(\vartheta_K) + \\ + 4\frac{kk_{\text{rw}}}{\mu\sqrt{\pi\alpha_w}} \sum_{\vartheta_j<t} A(\vartheta_j)(P_j - p_i)\left(\sqrt{t-\vartheta_j} - \sqrt{t-T_j^{\text{end}}}\right) + \\ + A(\vartheta_K)(P_K - p_i)\sqrt{t-\vartheta_K}. \tag{38}$$

Here P_j is the value of the pressure on the interval $[\vartheta_j, T_j^{\text{end}}]$ and P_K is the injection pressure on the current interval. The optimal value of P_K is obtained by minimization of functional (20) for $\vartheta = \vartheta_K$, $T = T_K$ with

$$a_q(t) = 4\frac{kk_{\text{rw}}}{\mu\sqrt{\pi\alpha_w}} A(\vartheta_K)\sqrt{t-\vartheta_K}, \tag{39}$$

$$b_q(t) = wA(\vartheta_K) + \\ + 4\frac{kk_{\text{rw}}}{\mu\sqrt{\pi\alpha_w}} \sum_{\vartheta_j<t} (P_j - p_i)A(\vartheta_j)\left(\sqrt{t-\vartheta_j} - \sqrt{t-T_j^{\text{end}}}\right). \tag{40}$$

Straightforward calculations produce the following result:

$$
\begin{aligned}
P_*^{\text{const}} \;=\; & p_i - \frac{1}{3}\frac{\mu\sqrt{\pi\alpha_w}}{kk_{\text{rw}}}\frac{1}{\sqrt{(t-\vartheta_K)}}w - \\
& - \frac{1}{2(T-\vartheta_K)^2 A(\vartheta_K)}\sum_{\vartheta_k<t}(P_*^k - p_i)A(\vartheta_k)\times \\
& \times\Bigg((2T-\vartheta_k-\vartheta_K)\sqrt{T-\vartheta_k}\sqrt{T-\vartheta_K} - \\
& - (\vartheta_K-\vartheta_k)^2\ln\left(\frac{\sqrt{T-\vartheta_K}+\sqrt{T-\vartheta_k}}{\sqrt{\vartheta_K-\vartheta_k}}\right) - \\
& - (2T-T_k^{\text{end}}-\vartheta_K)\sqrt{T-T_k^{\text{end}}}\sqrt{T-\vartheta_K} + \\
& + (\vartheta_K-T_k^{\text{end}})^2\ln\left(\frac{\sqrt{T-\vartheta_K}+\sqrt{T-T_k^{\text{end}}}}{\sqrt{\vartheta_K-T_k^{\text{end}}}}\right)\Bigg) + \\
& + \frac{1}{15}\frac{\mu\sqrt{\pi\alpha_w}}{kk_{\text{rw}}}\frac{1}{A(\vartheta_K)\sqrt{T-\vartheta_K}}[5Q_*(\vartheta_K)+3q_*(T-\vartheta_K)]. \qquad (41)
\end{aligned}
$$

The last formula provides a very simple method of computing the optimal constant injection pressure. It does not require any numerical integration, so the computation of (41) can be performed with very high precision.

3. Results

3.1. CONTROLLER SIMULATION AND IMPLEMENTATION

In this section we discuss several simulations of the controller. The computations below have been preformed using our controller simulator running under MS Windows.

In general, the controller implementation is described in Figure 1. As inputs, the controller needs the current measurements of the fracture area, the target cumulative injection, and the record of injection history. We admit that these data may be inaccurate, may have measurement errors, delays in measurements, etc. The controller processes these inputs and the optimal value of the injection pressure is produced on output. Based on the latter value, the wellhead valve is adjusted in order to set the injection pressure accordingly.

The stored measurements may grow excessively after a long period of operations and with many injectors. However, far history of injection pressure contributes very little to the integral on the right-hand side of Equation (1). Therefore, to calculate the current optimal control value, it is critical to know the history of injection parameters only on some time interval ending at the time of control planning, rather than the entire injection history. To estimate the length of such

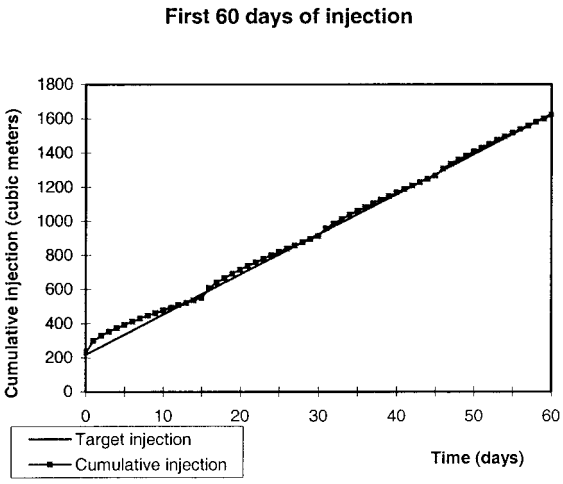

Figure 2. Target and optimal cumulative injection for a continuous fracture growth model.

interval, an analysis and a procedure similar to the ones developed in (Silin and Tsang, 2000) can be applied.

In our simulations we have used the following parameters. The absolute rock permeability, $k = 0.15$ md; the relative permeability of water $k_{\mathrm{rw}} = 0.1$; the water viscosity $\mu = 0.77 \times 10^{-3}$ Pa-s; the hydraulic diffusivity $\alpha_w = 0.0532\,\mathrm{m}^2$/Day; the initial reservoir pressure $p_i = 2.067 \times 10^4$ Pa; the target injection rate $q_* = 3.18 \times 10^5$ l/Day; and the fracture width $w = 0.0015$ m. These formation properties correspond to the diatomite layer G discussed in Part 1, Table I (Patzek and Silin, 2001). The controller has been simulated over a time period of 8 years. In the computations we have assumed that the initial area of a single fracture face A_0 is approximately equal to 900 square meters. Note that since the fracture surface may have numerous folds, ridges, forks etc., the effective fracture face area is greater than the area of its geometric outline. Therefore, the area of 900 square meters does not necessarily imply that the fracture face can be viewed simply as a 30-by-30 m square.

First, we simulate a continuous fracture growth model and the optimal injection pressure is obtained by solving the system of integral Equations (9) and (10). The length of the interval on which the optimal control was computed equals 20 days. Since we used 25% overlapping, the control was actually refreshed every 15 days. We assume that the fracture grows as the square root of time and its area approximately quadruples in 8 years. This growth rate agrees with the observations reported in Part 1.

Figure 2 shows that the cumulative injection produced by the optimal injection pressure, prescribed by the controller as in Figure 3, barely deviates from the target injection. The quasi-periodic oscillations of the slope are caused by the interval-wise design of control.

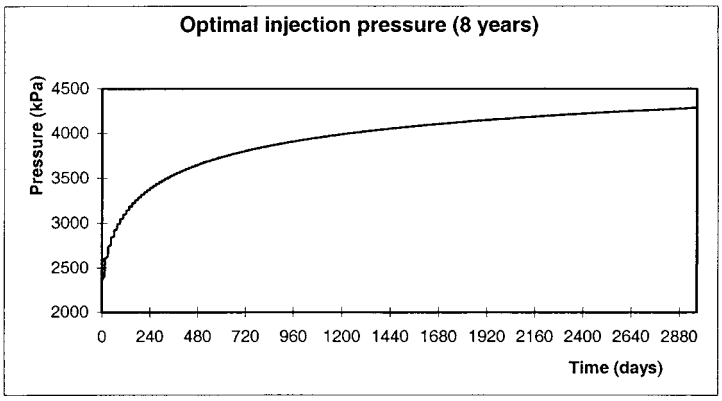

Figure 3. The optimal injection pressure for a continuous square-root-of time fracture growth model.

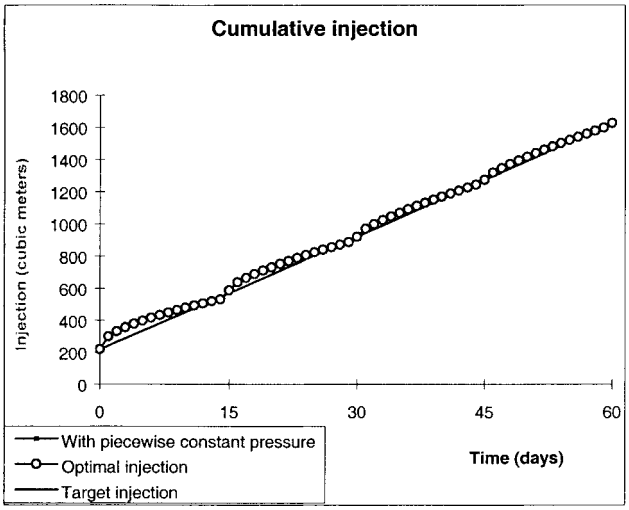

Figure 4. Cumulative injection in piecewise constant and continuous control modes.

A comparison of piecewise constant pressure with the optimal pressure in continuous mode (see Equation (21) and Equations (9) and (10), respectively) results in a difference of less than 1%. The respective cumulative injection is almost the same as the one found for the continuous pressure mode.

For a piecewise constant fracture growth model the simulation results remain basically the same. The cumulative injection during the first 60 days is shown in Figure 4. Again, one observes a vanishing oscillatory behavior of the slope caused by refreshing the control every 15 days. The pressures are plotted in Figure 5. The piecewise constant pressure computed using the explicit formula in Equation (41) only slightly differs from the optimal pressure obtained by solving the system of Equations (33) and (34).

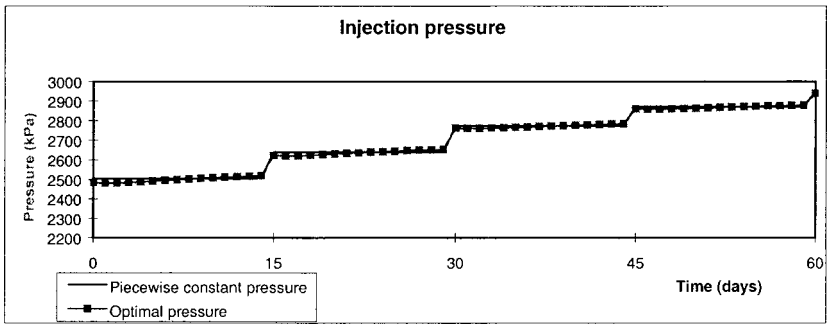

Figure 5. Comparison between piecewise constant and continuous mode of control: piecewise constant fracture growth model.

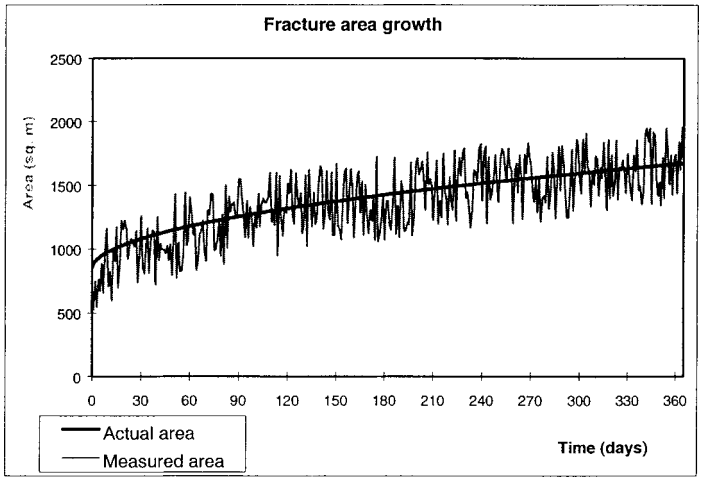

Figure 6. Fracture area is measured with a random error.

We do not show the cumulative injection produced by the exactly optimal pressure because by construction it coincides with the target injection.

In the simulations above, we have assumed that all necessary input data are available with perfect accuracy. This is a highly idealized choice, only to demonstrate the controller performance without interference of disturbances and delays. Now let us assume that the measurements become available with a 15-day delay, which in our case equals one period of control planning. Also assume that the measurements are disturbed by noise which is modeled by adding a random component to the fracture area. Thus, as the controller input we have $A(t - 15 \text{ days delay}) + \text{error}(t)$, instead of $A(t)$. In this manner we have introduced both random and systematic errors into the measurements of the fracture area. The range of $\text{error}(t)$ is about 40% of the initial fracture face area $A(0)$. Figure 6 shows the actual and the observed fracture area growth.

The performance of the controller is illustrated in Figure 7. Again, the distinction between the injection produced by the optimal pressure and the injection

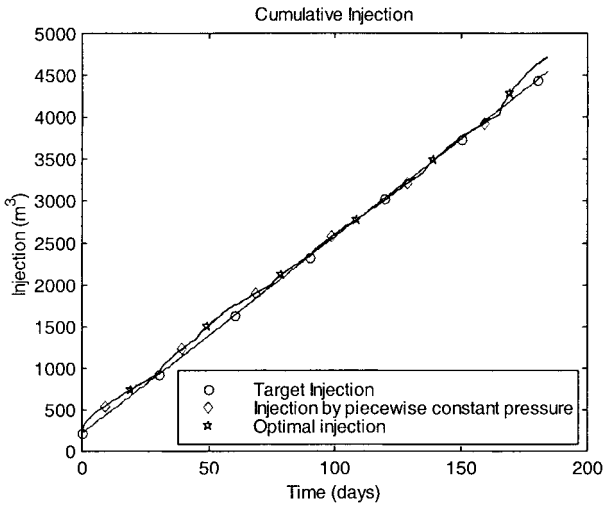

Figure 7. Comparison between the cumulative injection produced by two modes of optimal control and the target injection.

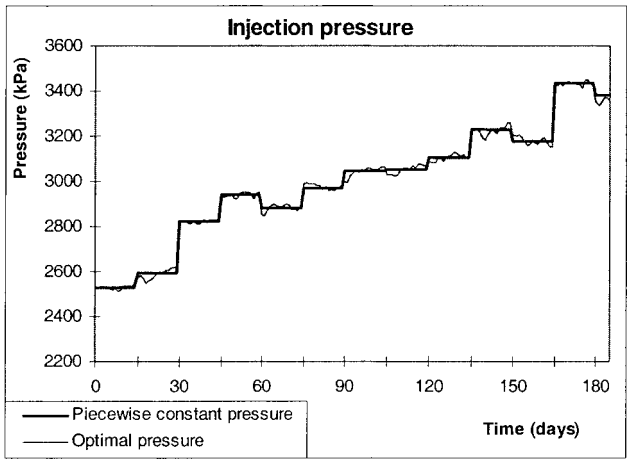

Figure 8. Two modes of optimal injection pressure.

produced by piecewise constant optimal pressure is hardly visible. The difference between the target injection and the injection produced by the controller is still small. The injection pressure during the first six months is shown in Figure 8. Again, the piecewise constant pressure and the pressure obtained by solving the system of integral Equations (9) and (10) do not differ much.

Now, let us consider a situation where at certain moments the fracture may experience sudden and large extensions. In the forthcoming example, the fracture experienced three extensions during the first 3 years of injection. On the 152nd day of injection its area momentarily increased by 80%, on the 545th day it increased by 50%, and on the 1004th day it further increased by another 30% (see Figure 9). In

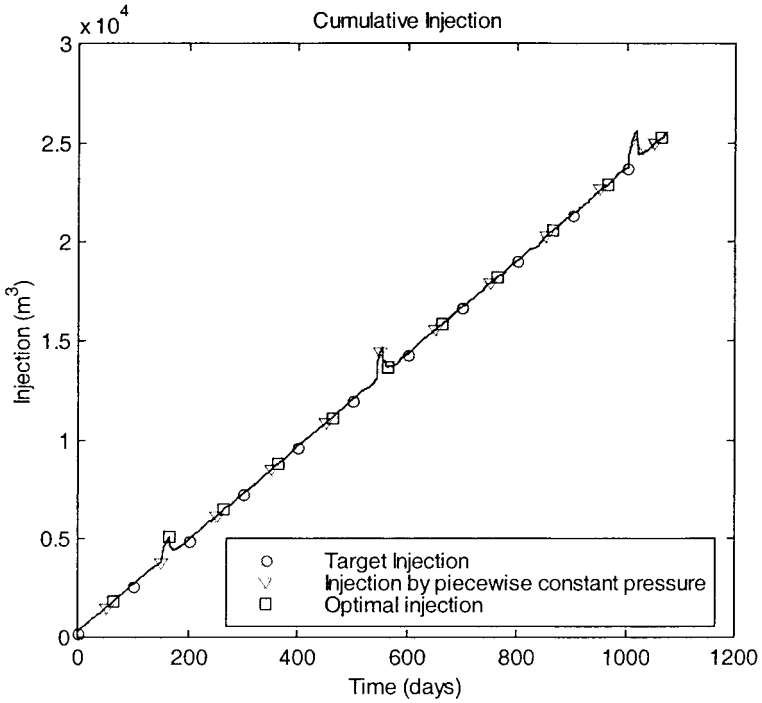

Figure 9. Cumulative injection experiences perturbations at fracture extensions and then returns to a stable performance by the controller.

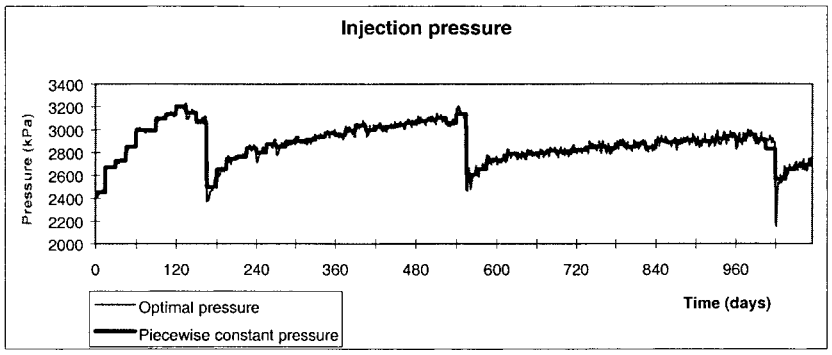

Figure 10. Two modes of optimal injection pressure in presence of fracture extensions.

the simulation the measurements were available with a 15-day delay and perturbed with a random error of up to 40% of $A(0)$. At each moment of the fracture extension the controller reacted correctly and decreased the injection pressure accordingly, Figure 10. The optimal pressure obtained from the solution to the system of integral Equations (9) and (10) is more stable and the piecewise constant optimal pressure does not reflect the oscillations in the measurements due to its nature. The resulting

cumulative injection also demonstrates stability with respect to the oscillations in the measurements. However, the injection rate, which is equal to the slope of the cumulative injection experiences abrupt changes, see Figure 9.

The exactly optimal injection pressure presented in Equation (26) is obtained by solving an integral Equation (1) with respect to $p_{\text{inj}}(t)$. The main difficulty with implementation of this solution is that we need to know not only the fracture area, but its growth rate $\mathrm{d}A(t)/\mathrm{d}t$ as well. Clearly, the latter parameter is extremely sensitive to measurement errors. In a continuous fracture growth model, an interpolation technique can be applied for estimating the extension rate. In a piecewise constant fracture growth model, Equation (26) reduces to a much simpler Equation (36). Therefore, in such a case the exactly optimal injection pressure can be obtained with little effort. However, since exactly optimal control is designed on entire time interval, from the very beginning of the operations, its performance can be strongly affected by perturbations in the input parameters caused by measurements errors. Moreover, each fracture extension is accompanied by a singularity in Equation (36). Therefore, a control given by Equation (26) or Equation (36) can be used for qualitative studies, or as the function $p_*(t)$ in criterion (3), rather than for a straightforward implementation.

4. Model Inversion into Fracture Area

As we remarked in the Introduction, the effective fracture area $A(t)$ is the most difficult to obtain input parameter. The existing methods of its evaluation are both inaccurate and expensive. However, the controller itself is based upon a model and this model can be inverted in order to provide an estimate of $A(t)$. Namely, Equation (1) can be solved with respect to $A(t)$. This solution can be used for designing the next control interval and passed to the controller for computing the injection pressure. If a substantial deviation of the computed injection rate from the actual one occurs, the control interval needs to be refreshed while the length of the extrapolation interval is kept small.

An obvious drawback of such an algorithm is the necessity of planning the control to the future. At the same time, as we have demonstrated above, a delay in the controller input is not detrimental to its performance if the control interval is small enough. Automated collection of data would reduce this delay to a value that results in definitely better performance than could be achieved with manual operations.

For a better fracture and formation properties status estimation a procedure similar to the well operations data analysis method developed in (Silin and Tsang, 2000) can be used. We will address this issue in more detail elsewhere. Here we just present an example of straightforward estimation algorithm based on Equation (1), Figure 11. Figure 11(a) shows the plot of cumulative injection, Figure 11(b) shows the injection pressure during 700 days of injection. The plot in Figure 11(c) shows the calculated relative fracture area, that is the dimensionless area relative to the

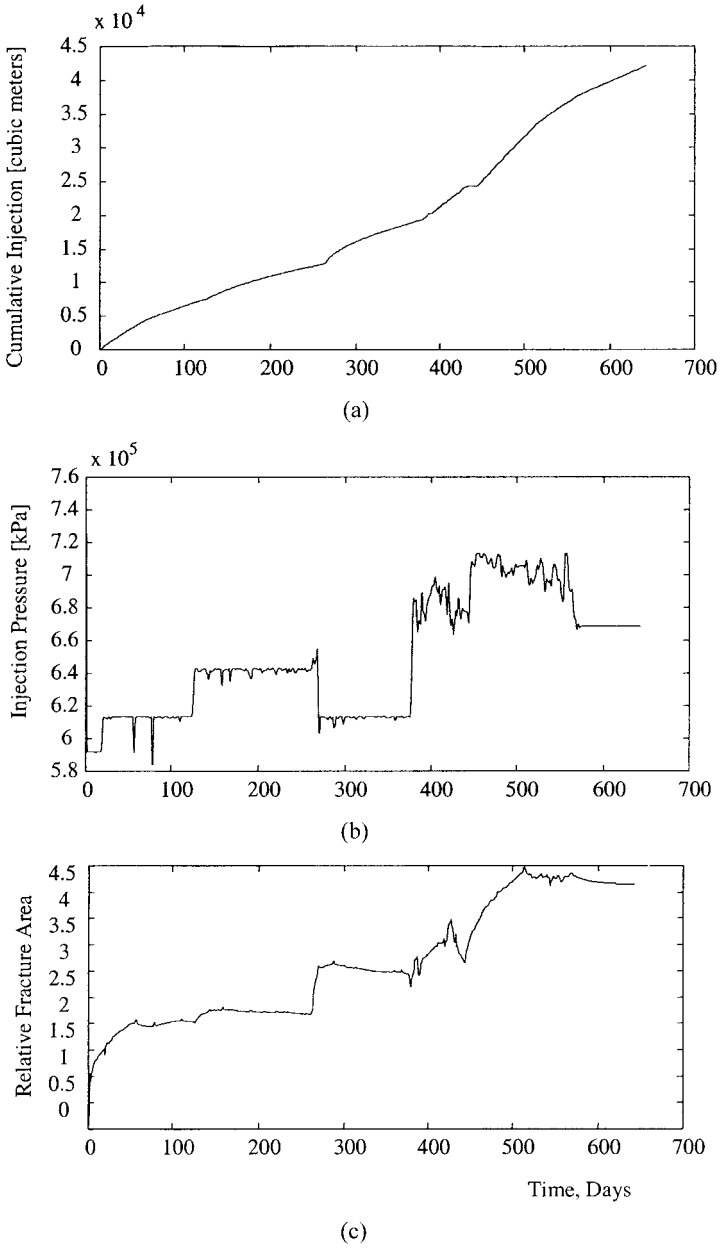

Figure 11. Straightforward fracture growth estimation.

initial value. One can see that noticeable changes in injection conditions and hydrofracture status occurred between 200 and 300 days and after 400 hundred days of injection.

The advantage of the proposed procedure is in its cost. Because the injection and injection pressure data are collected anyway, the effective fracture area is obtained

'free of charge'. In addition, the computed estimate of the area is based on the same model as the controller, so it is exactly the required input parameter.

5. Conclusions

A control model of water injection into a low-permeability formation has been developed. The model is based on Part 1 of this paper (Patzek and Silin, 2001), where the mass balance of fluid injected through a growing hydrofracture into a low-permeability formation has been investigated. The input parameters of the controller are the injection pressure, the injection rate and an effective fracture area. The output parameter is the injection pressure which can be regulated by opening and closing the valve at the wellhead.

The controller is designed using principles of the optimal control theory. The objective criterion is a quadratic functional with a stabilizing term. The current optimal injection pressure depends not only on the current instantaneous measurements of the input parameters, but on the entire history of injection. Therefore, a genuine closed loop feedback control mode impossible. A procedure of control design on a relatively short sliding interval has been proposed. The sliding interval approach produces almost a closed loop control.

Several modes of control and several models of fracture growth have been studied. For each case a system of equations characterizing the optimal injection control has been obtained. The features affecting the solvability of such a system have been studied. We demonstrate that the pair of forward and adjoint systems can be represented in an operator form with a symmetric and positive definite operator. Therefore, the equations can be efficiently solved using standard iterative methods, for example, the method of conjugate gradients.

The controller has been implemented as a computer simulator. The stable performance of the controller has been illustrated by examples. A procedure for inversion of the control model for estimating the effective fracture are has been proposed.

Acknowledgements

The authors are thankful to the anonymous reviewers for their valuable remarks and suggestions. This work was supported in part by two members of the U.C. Oil® Consortium, Chevron Petroleum Technology Company, and CalResources (now Aera Energy), LLC. Partial support was also provided by the Assistant Secretary for Fossil Energy, Office of Gas and Petroleum Technology, under contract No. DE-ACO3-76FS00098 to the Lawrence Berkeley National Laboratory of the University of California. We thank CalResources for releasing the Phase II steam pilot data, and Crutcher-Tufts for releasing the Dow-Chanslor waterflood data. We also thank Mobil E&P US for providing the Lost Hills I waterflood data.

References

Ashour, A. A. and Yew, C. H.: 1996, A study of the fracture impedance method, In: *47th Annual CIM Petroleum Society Technical Meeting*, Calgary, Canada.

Barkman, J. H. and Davidson, D. H.: 1972, Measuring water quality and predicting well impairment, *J. Pet. Tech.* **7**, 865–873.

De, A. and Patzek, T. W.: *Waterflood Analyzer, MatLab Software Package*, Version 1.0, 1999. Lawrence Berkley National Laboratory, Berkeley, CA.

Holzhausen, G. R. and Gooch, R. P.: 1985, Impedance of hydraulic fractures: Its measurement and use for estimating fracture closure pressure and dimensions, In: *SPE/DOE 1985 Conference on Low Permeability Gas Reservoirs*, SPE, Denver, CO.

Howard, G. C. and Fast, C. R.: 1957, Optimum fluid characteristics for fracture extension, *Drill. Prod. Prac. API* 261–270.

Kolmogorov, A. N. and Fomin, S. V.: 1975, *Introductory Real Analysis*, Dover Publications, New York.

Patzek, T. W. and De, A.: 1998, Lossy transmission line model of hydrofactured well dynamics, In: *1998 SPE Western Regional Meeting*, Bakersfield, SPE, CA.

Patzek, T. W. and Silin, D. B.: Water injection into a low- permeability rock – 1. Hydrofracture growth. This Journal, 2001.

Silin, D. B. and Tsang, C.-F.: 2000, *Identification of Formation Properties from Operations Data*, Lawrence Berkeley National Laboratory, Rep. LBNL-45079 Berkeley, CA.

Tikhonov, A. N. and Arsenin, V. Y.: 1977, *Solutions of Ill-Posed Problems*, Scripta series in mathematics, Halsted Press, New York.

Vasil'ev, F. P.: 1982, *Numerical Methods for Solving Extremal Problems* (in Russian), Nauka, Moscow.

Warpinski, N. R.: 1996, Hydraulic fracture diagnostics, *J. Petrol. Tech.* **10**.

Wright, C. A. and Conant, R. A.: 1995, SPE 30484, hydraulic fracture reorientation in primary and secondary recovery from low-permeability reservoirs, In: *SPE Annual Technical Conference & Exhibition*, Dallas, TX.